Available *online* at: http://journal.unj.ac.id

Jurnal Pensil Pendidikan Teknik Sipil

Journal homepage: http://journal.unj.ac.id/unj/index.php/jpensil/index

NUMERICAL ANALYSIS OF WINDOW OPENINGS AS VENTILATION FOR 3-STOREY BUILDINGS IN A TROPICAL AREA

Okky Hendra Hermawan[1*], *Laksana Putra Ramadhan*[2], *Irfan Santosa*[3]

[1,2] Department Civil Engineering, Faculty of Engineering and Computer Science, Universitas Pancasakti Tegal, Indonesia

Jl. Halmahera KM. 01, Mintaragen, East Tegal, Tegal City, Central Java, 52121, Indonesia

3Department Mechanical Engineering, Faculty of Engineering and Computer Science, Universitas Pancasakti Tegal, Indonesia

Jl. Halmahera KM. 01, Mintaragen, East Tegal, Tegal City, Central Java, 52121, Indonesia

[*1]okky_hendra@upstegal.ac.id, [2]laksanaputra977@gmail.com, [3]irfansantosa@upstegal.ac.id

P-ISSN: 2301-8437
E-ISSN: 2623-1085

ARTICLE HISTORY
Accepted:
10 Juli 2025
Revision:
24 September 2025
Published:
30 September 2025

ARTICLE DOI:
10.21009/jpensil.v13i3.48630

Abstract

Building form has a significant influence on energy efficiency, especially in tropical regions where minimizing cooling demand is crucial. Natural ventilation is widely recognized as a passive strategy to reduce energy use while maintaining indoor comfort; however, limited research has integrated experimental validation and CFD analysis in tropical institutional buildings. This study investigates the effect of window openings on airflow and thermal distribution in a three-story library building in Pemalang, Central Java, Indonesia. Field measurements and CFD simulations were conducted, with validation showing good agreement (RMSE = 0.69). Results indicated that while the first floor achieved adequate circulation and stable temperatures, the upper floors experienced stagnation zones and higher indoor heat accumulation, suggesting suboptimal natural ventilation. Parametric simulations demonstrated that square pivot windows at 60° and 90° provided the most effective performance, improving airflow and reducing indoor temperatures. The findings highlight the importance of optimized window design as a passive cooling strategy to enhance thermal comfort and energy efficiency in tropical buildings without reliance on mechanical systems.

Keywords: Natural ventilation, Window design, 3-Story Building, CFD Simulation

Introduction

The tropics are defined as the area between the northern latitudes of the Tropic of Cancer (approximately 23°26' N) and the southern latitudes of the Tropic of Capricorn (approximately 23°26' S). Based on the Köppen-Geiger classification, the main climate types found in the tropics include tropical rainforest climate, tropical monsoon climate, tropical wet and dry (savanna) climate, tropical desert climate, and subtropical climate. (Sarmento, 2012). The average daily temperature ranges from 30 °C to 38 °C with low rainfall and intense solar radiation. (Feeley & Stroud, 2018) & (M. C. Peel1, B. L. Finlayson2, 2002). Indonesia is a tropical country that experiences two main seasons: the rainy season and the dry season, which are characterized by low humidity and high temperatures. These climatic conditions indicate that building form plays an important role in achieving energy efficiency, especially in tropical areas. However, the influence of building form on energy savings has only begun to receive significant attention in the last decade (Chung-Camargo et al., 2024). Natural ventilation is a solution that can reduce energy consumption and operational costs while increasing physical and psychological comfort. (Mora-Pérez et al., 2017), (Elhassan, 2023), (Sakiyama et al., 2020), (Rodrigues et al., 2019), (Awoyera et al., 2024). Buildings with natural ventilation offer better user control and environmental quality than buildings with mechanical ventilation. (de Dear & Brager, 2002). Exposure to heat and confined spaces can cause sick building syndrome in occupants, leading to negative perceptions of the building. (Wen et al., 2020). Since many air-conditioned buildings do not have a dedicated fresh air system, occupants often open windows to get fresh air with one-sided natural ventilation. (Roetzel et al., 2010), (Park & Choi, 2019), (Gu et al., 2021), and (Hargianti et al., 2023). A survey of 303 office workers showed that 66% of them regularly open windows, and another 19% do so occasionally. (Nisiforou et al., 2012). In control strategies, the combination of mechanical and natural ventilation systems is referred to as 'concurrent' ventilation mode. (Ai & Mak, 2016). To make it clearer, we describe it as natural ventilation through window openings in an air-conditioned room. This ventilation approach can improve indoor air quality if the outdoor air is clean (Chenari et al., 2016). However, this ventilation also causes the cold air inside the room to escape quickly during the summer, before the residual heat can be effectively removed, which ultimately increases energy consumption. (L. Wang & Greenberg, 2015). Although many studies have analyzed and predicted user behavior in opening windows (Haldi & Robinson, 2008), predicting ventilation performance accurately remains a major challenge. This is due to the complex influence of various factors on indoor airflow distribution, including the placement of air intakes, window openings, and the dynamic interaction between indoor and outdoor environments. (S. Liu et al., 2019), (Cao, 2019), (Yin et al., 2024), (Bachand et al., 2025) . Natural ventilation can be analyzed using three main approaches: empirical models, experimental measurements, and CFD simulations. Empirical models, which are generally derived from the orifice equation and Bernoulli's principle, provide a rapid estimate of the ventilation rate. (H. Wang & Chen, 2012). As an example, Grabe (Von Grabe, 2013), Caciolo (Caciolo et al., 2013), and Liu (X. Liu et al., 2024) each proposed an empirical model to study one-sided natural ventilation. However, these models often have a high degree of uncertainty due to simplifications in representing the interaction between wind pressure and thermal pressure, as well as limitations related to the characteristics of a particular building. (Wen et al., 2024), (Conzatti et al., 2025), (Bogdan Cfd et al., 2017).

To address this gap, the Pemalang Regency Library Building in Central Java, Indonesia, was selected as the case study. The building's distinctive architectural form, three-story spatial configuration, and use of pivot windows provide unique conditions for examining the interaction between window openings, airflow distribution, and temperature patterns. As a public facility accommodating large numbers of users daily, effective natural ventilation is essential to ensure both thermal comfort and acceptable indoor air quality. These features make the building a representative and academically relevant object of study, with findings transferable to similar tropical public facilities. This study aims to investigate the effect of ventilation models and window opening configurations on the performance of natural ventilation in a three-story library building.

Experimental field measurements of temperature and air velocity (Palomo Amores et al., 2025) were conducted, complemented by CFD modeling (Hawendi & Gao, 2017). The CFD model employed boundary conditions derived from the experiments, with its accuracy verified using error analysis. The novelty of this research lies in the integrated experimental–numerical evaluation of pivot window configurations in a tropical multi-story public building, providing new insights into passive cooling strategies applicable to institutional facilities in hot-humid climates.

Research Methods

This research adopts a case study approach focusing on a three-story library building in Pemalang, Indonesia, to analyze temperature distribution and airflow patterns under different window configurations. Field measurements of air temperature were conducted at the midpoint of each floor, 1.1 m above the floor level (representing the breathing zone), during typical operating hours. Data loggers with an accuracy of ±0.5 °C recorded the values at 5-minute intervals, and the results were subsequently used as boundary conditions for computational fluid dynamics (CFD) simulations (Chen & Gorlé, 2022). The numerical simulations were performed using the SST k-ω turbulence model (Demir, 2025), testing two window geometries with variations in orientation and opening angle. A structured mesh was applied, and grid independence was verified to ensure solution stability. Validation of the CFD results was carried out by comparing simulated temperatures with experimental measurements using Root Mean Square Error (RMSE) analysis. To evaluate the effectiveness of ventilation design, the proportion of floor area maintaining temperatures below 27.15 °C—corresponding to the upper limit of thermal comfort (BSN, 2001), (ASHRAE 55, 2020)—was calculated for the second (440 m²) and third floors (292 m²). This percentage served as a quantitative indicator of the effectiveness of each window configuration in improving indoor thermal comfort.

Geometry

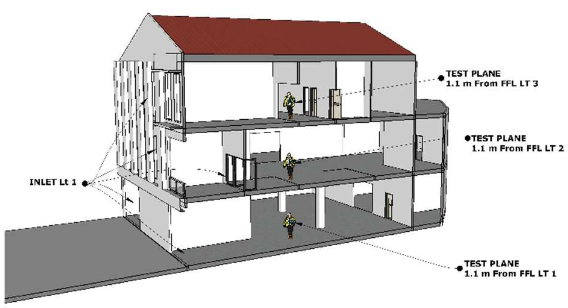

(a) (b)

Figure 1. (a) Building geometry and measurement points, (b) Existing Pemalang Library building

The building geometry and measurement points are shown in Fig. 1 (a), and the existing condition of the Pemalang library building is shown in Fig. 1 (b). The rooms on the 1st and 2nd floors have an area of 440 m² with a left length of 29.55 m x right length of 18 m x width of 16.5 m x and a height of 3.6 m. while the 3rd floor has an area of 292 m², with a length of 18 m x width of 16.5 m. Air temperature measurements were carried out at the center point of the building at a height of 1.1 meters from the surface of each floor.

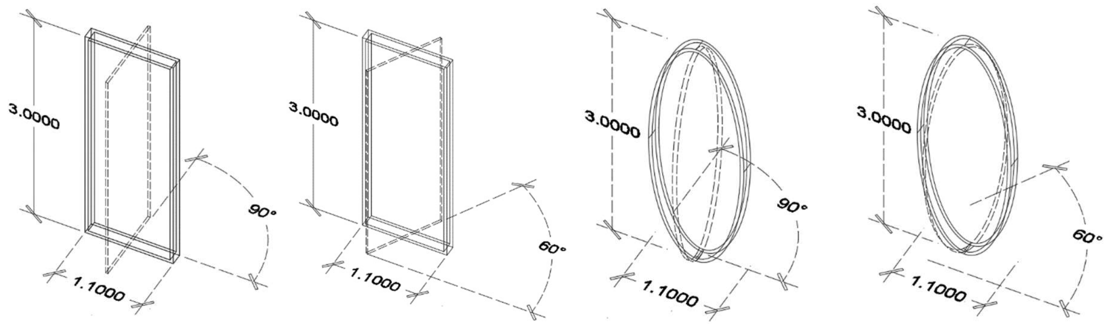

Figure 2. window geometry (a) Rectangle 90°, (b) Rectangle 60°, (c) Oval 90°, (d) Oval 60°

Ventilation uses 3 × 1.1 meter windows located on the 2nd and 3rd floors, with 8 windows on the 2nd floor and 15 windows on the 3rd floor. The distance between the building and the surrounding buildings is 0.5 meters on the right side and 1 meter on the left side. Field experiments and CFD simulations were conducted on two window geometry models with variations in orientation angles and opening percentages to analyze the effect of openings on indoor air temperature, as shown in Figure 2.

Table 1. Temperature and Air Velocity in the Library Building

Time	Floor 1st		Floor 2nd		Floor 3rd	
	Temperature °C	Air velocity m/s	Temperature °C	Air velocity m/s	Temperature °C	Air velocity m/s
08.00 - 09.30	27,8 - 28,9	0,25 - 0,6	28,5 - 30	0,7 - 1,2	29 - 31	0,9 - 2,2
13.00 - 14.00	29,2 - 29,8	0,7 - 0,9	30,2 - 31	0,9 - 1,4	31,7 - 32,8	1,7 - 2,1
15.30 - 16.00	28, - 29	0,5 - 0,9	29,8 - 30	1,2 - 1,4	30,2 - 31	0,7 - 2,1

As shown in Table 1, the recorded temperature and air velocity reflect the indoor–outdoor conditions of the Pemalang Library building. Measurements were conducted during the library building's operating hours, namely between 08.00 and 16.00. The measurement duration ranged from 30 to 60 minutes, depending on the room temperature fluctuation. Temperature measurements were conducted indoors on each floor, while air velocity measurements were conducted outdoors at each floor height. For the simulation in this study, the highest temperature data that occurred in the time range from 11.00 to 14.00 were used, as well as the highest air velocity data at each floor height.

Mathematical Model and Solver Settings

The Reynolds-averaged Navier-Stokes (RANS) equations modified by SST k-Omega have the ability to accommodate long, straight fluid flows, such as in wide free stream areas, and have the advantage of increasing their accuracy in areas with detailed flow. (Menter, 1994).
SST K-Omega Turbulent Equation:

1. *Transport Equation for Turbulent Kinetic Energy (k)*

$$\partial \frac{(\rho k)}{\partial t} + \frac{\partial(\rho u j k)}{\partial x j} = P - \beta^{*} \rho \omega k + \frac{\partial}{\partial x j} \left[(\mu + \sigma_k \mu_t \frac{\partial k}{\partial j} \right] \quad (1)$$

2. *Transport Equation for Specific Dissipation Rate (ω / omega)*

$$\partial \frac{(\rho\omega)}{\partial t} + \frac{\partial(\rho uj\omega)}{\partial xj} = \frac{\gamma}{\nu_t} P \ - \beta\rho\omega^2 + \frac{\partial}{\partial xj} \ \left[(\mu + \ \sigma_\omega \mu_t \ \frac{\partial\omega}{\partial\chi j}\right] + 2(1 - F_1) \frac{\rho\sigma_{\omega 2}}{\omega} \frac{\partial\kappa}{\partial xj} \frac{\partial\omega}{\partial xj} \quad (2)$$

3. *Turbulent Viscosity (μ_t)*

$$\mu_t \frac{\rho\alpha_1\kappa}{max\ (\alpha_1\omega, SF_2,} \quad (3)$$

Boundary Conditions

In this simulation, boundary conditions are set based on field conditions to accurately represent the physical environment. The domain includes a windowed building and its surrounding free-flow area, with a clearance of 50 cm on the right side and 100 cm on the left side. The front side is the velocity inlet, the right, left, and top sides are assumed to be free flow, and the bottom side is the no-slip wall. Room partitions and windows are obstacles, as shown in Table 2.

Table 2. Boundary Conditions For Simulation

Item	Boundary Condition Setting
inlet	Temperature: 27 C° Velocity : Floor 1 : 0.9 m/s, Floor 2 : 1.4 m/s, Floor 3:2,2 m/s.
outlet	Outflow
window	No Slip Condition
wall	No Slip Condition
Wall Function	Standard Wall Function
Initial room temperature	Temperature Lt 1 : 29 °C, Lt 2 : 30 °C, Lt 2 : 32 °C
Turbulence model	Standar SST K-Omg model
Other Parameter	Software Default Value

Research Results and Discussion

Simulation Validation and Error Analysis

To ensure the reliability of the CFD modeling results, a Grid Independence Test (GIT) was performed to verify that the simulation results were not affected by the mesh size or density (Lee et al., 2020). Testing was carried out up to 7 iterations, with the number of elements varying between 60,000 and 120,000. The main parameter observed was the air temperature inside the runner chamber.

When the number of elements exceeds 90,000, the temperature value begins to approach stability and shows the lowest difference in the Grid Independence Test (GIT), which is 1.1%, as shown in Figure 3. Therefore, the simulation configuration with the number of elements as many as 90,000 is used as the main reference for the entire simulation process.

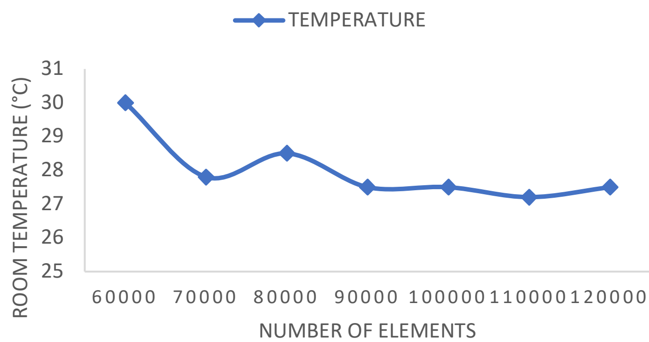

Figure 3. Grid Independence Test Graph *(GIT)*

Temperature Distribution and Flow Pattern in Existing Building Spaces

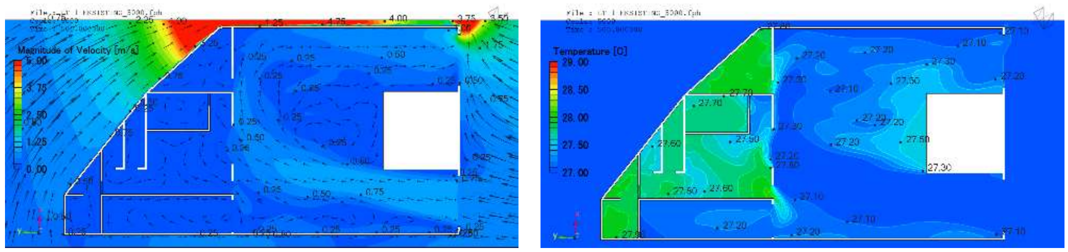

(a) (b)

Figure 4. Existing Result Floor 1 (a) Velocity, (b) Temperature

Based on the simulation results as shown in Figure 4 (a) and (b), the air flow in the existing condition of the 1st floor shows the highest speed reaching 5 m/s on the right side outside the building, while inside the room it ranges between 0.25–0.75 m/s. The flow pattern forms several vortices, indicating the presence of local circulation at low speed. The temperature distribution in the room is relatively even, between 27.1 °C and 27.9 °C, indicating that the air circulation is sufficient to maintain thermal stability. However, the air flow in the room tends to be slow, so there is a risk of creating areas with suboptimal air exchange.

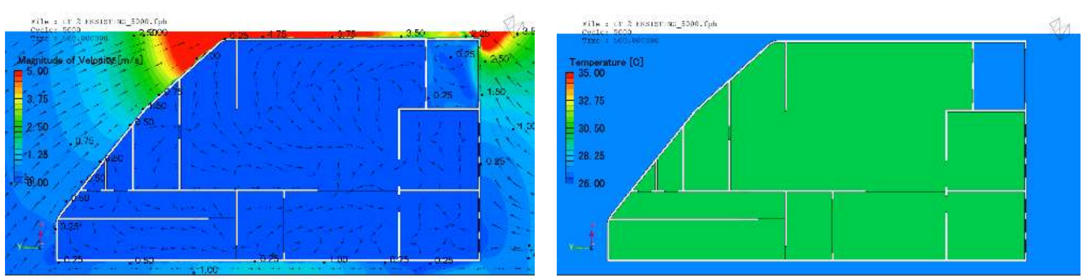

(a) (b)

Figure 5. Existing Result Floor 2 (a) Velocity, (b) Temperature

Based on the simulation results in Figure 5 (a) and (b), the airflow on the 2nd floor is mostly stagnant, with velocities below 0.25 m/s and small eddies, while the highest velocity (5 m/s) occurs only on the right side of the building. The uniform color of the velocity contour indicates low heat transfer and ineffective natural ventilation. The indoor temperature is relatively uniform at 30–32 °C, except on the balcony (27 °C), indicating the accumulation of warm air inside the building.

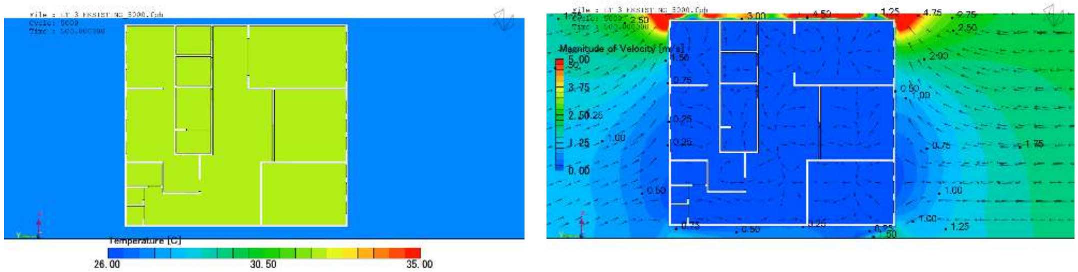

(a) (b)

Figure 6. Existing Result Floor 3 (a) Velocity, (b) Temperature

Based on the simulation results as shown in Figure 6 (a) and (b), the air flow on the 3rd floor is stagnant, with a velocity below 0.25 m/s and the formation of small eddies. The maximum velocity of 5 m/s only occurs on the right side of the outside of the building. This condition reflects less effective natural ventilation, so that warm air is trapped indoors. The temperature distribution is relatively even in the range of 30–32 °C, with minimal color gradation indicating low heat transfer due to the absence of adequate air flow.

Temperature Distribution and Flow Patterns in Building Spaces With Case Windows Opening Models 1

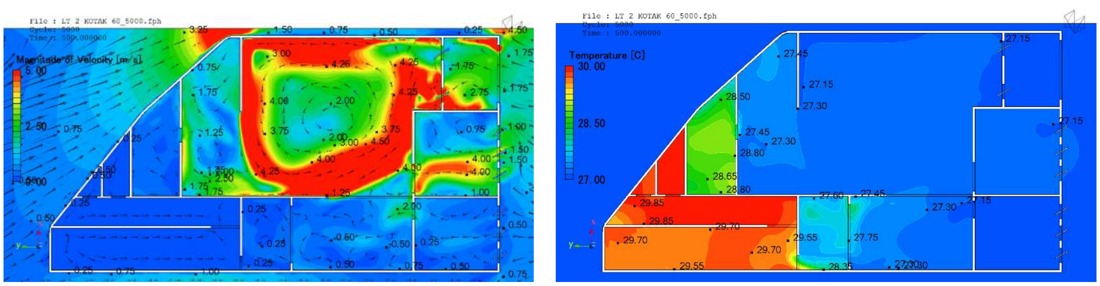

(a) (b)

Figure 7. Result Floor 2 Case 1 Angle 60° (a) Velocity, (b) Temperature.

Based on the simulation results shown in Figure 7 (a) and (b), the air flow on the 2nd floor has the highest velocity (≥4 m/s) in the middle right part of the room, while low velocity (<0.5 m/s) occurs in the corner and the left rear area which is potentially stagnant. The air vortex pattern indicates flow mixing. The temperature distribution ranges from 27–30 °C, with heat accumulation in the rear area (up to 30 °C) due to limited circulation, and the lowest temperature (27–27.15 °C) is observed in the front part of the room due to optimal air supply from the window.

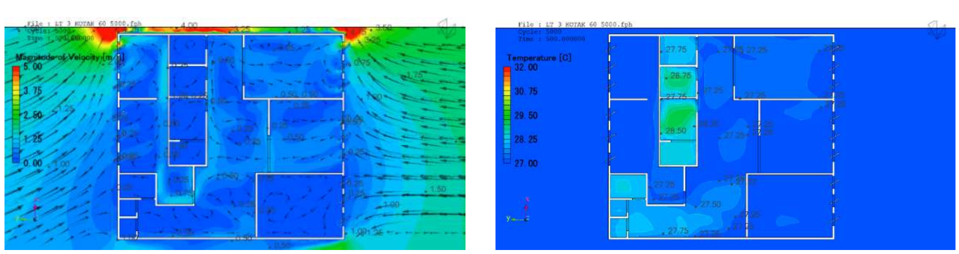

(a) (b)

Figure 8. Result Floor 3 Case 1 Angle 60° (a) Velocity, (b) Temperature

Based on the simulation results shown in Figure 8 (a) and (b), the air flow on the 3rd floor shows the highest velocity (≥4 m/s) in the outer corridor area, while the slow flow (<0.5 m/s) is evenly distributed inside the room. The temperature distribution is dominated by the range of 27–27.25°C, with the highest temperature (28.75°C) observed in the small central room due to minimal circulation, and the lowest temperature (27°C) in the front room as a result of optimal air supply through the window.

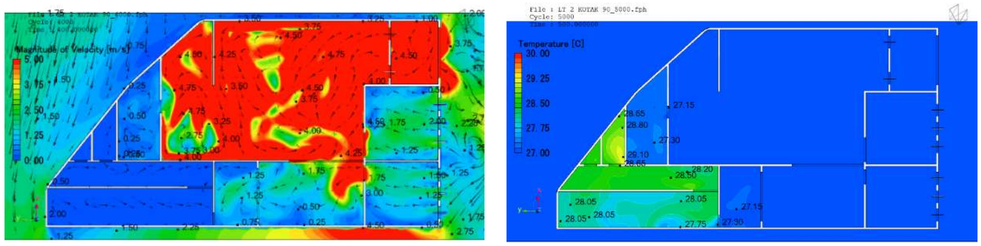

(a) (b)

Figure 9. Result Floor 2 Case 1 Angle 90° (a) Velocity, (b) Temperature.

Based on the simulation results shown in Figure 9 (a) and (b), the air flow on the 2nd floor of Case 1, 90° Angle is uneven, with the highest speed (4.75 m/s) in the middle right of the room and low velocity (<1 m/s) in the rear area and separate room. The inflow from the front right spreads turbulently, but does not reach the entire room, thus triggering a stagnant zone and potential thermal discomfort. The temperature distribution is dominated by the range of 27–28.80°C, with heat accumulation (up to 29.10°C) on the left rear side due to limited circulation, and the front and middle areas are cooler (27–27.15°C) due to more effective air flow.

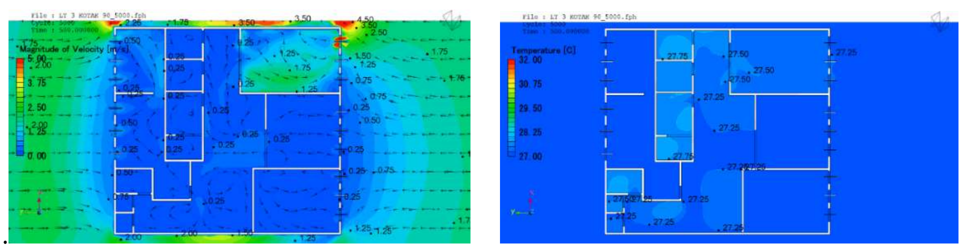

(a) (b)

Figure 10. Result Floor 3 Case 1 Angle 90° (a) Velocity, (b) Temperature

Based on the simulation results as shown in Figure 10 (a) and (b), it shows the air velocity flow entering from the front with an initial speed of 1.4 m/s and a maximum of 5 m/s in the left aisle due to the vortex. Most of the rooms have low velocities (0–0.75 m/s), with local circulation at several points. High velocities tend to appear near the openings, while closed areas experience stagnation. The room temperature distribution is relatively stable in the range of 27–27.20°C, with a slight increase (up to 27.75°C) in the middle area. The dominance of the light blue color indicates that ventilation is quite effective in maintaining an even temperature without significant hotspots at 500 seconds.

Temperature Distribution and Flow Pattern in Building Spaces With Case Windows Opening Models 2

Based on the simulation results as shown in Figure 11 (a) and (b), the air velocity flow is uneven, with the highest velocity (3.5–5 m/s) in the front center of the room and slow flow (<1 m/s) on the left side and separate rooms. The inflow from the front center spreads with turbulence, but does not reach the entire area, causing potential stagnation and thermal discomfort. The room temperature distribution is 27–30°C, with the highest temperature (up to 30°C) at the back due to minimal air circulation. On the contrary, the lowest temperature (27–27.15°C) is found in the front and middle areas due to effective natural ventilation. This temperature imbalance is caused by the absence of an outlet, which triggers heat accumulation at the back.

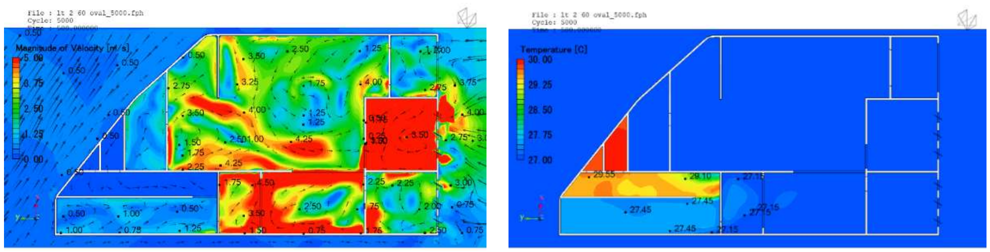

(a) (b)

Figure 11. Result Floor 2 Case 2 Angle 60° (a) Velocity, (b) Temperature

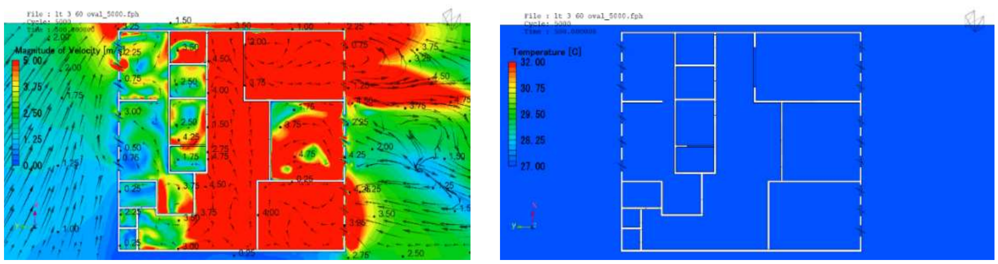

(a) (b)

Figure 12. Result Floor 3 Case 2 Angle 60° (a) Velocity, (b) Temperature.

Based on the simulation results as shown in Figure 12 (a) and (b), the air flow is evenly distributed, with the highest velocity (3.5–5 m/s) in the front center and low velocity (<1 m/s) in the rear area. The inflow from the front spreads with turbulence and potential vortex formation. The temperature distribution is uniform in the range of 27°C, without excessive hot areas. This indicates that heat transfer is evenly and efficiently throughout the room.

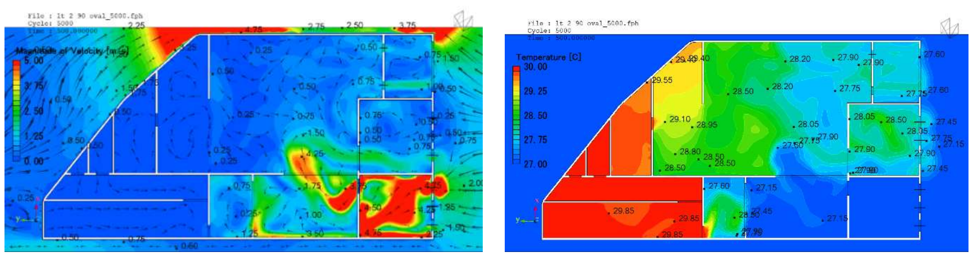

(a) (b)

Figure 13. Result Floor 2 Case 2 Angle 90° (a) Velocity, (b) Temperature

Based on the simulation results as shown in Figure 13 (a) and (b), the air flow on the 2nd floor is uneven, with high velocity (4.5–5 m/s) on the front left and low (<1 m/s) in most rooms, triggering turbulence and potential stagnation. The temperature distribution shows 27–30°C, the highest temperature is in the back room due to a lack of circulation and outlet, while the lowest temperature is on the front left as the air inlet.

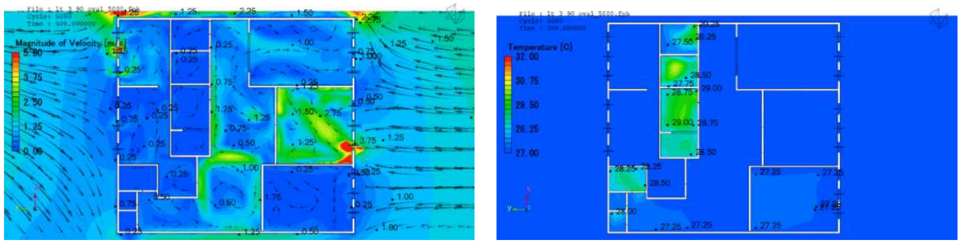

(a) (b)

Figure 14. Result Floor 3 Case 2 Angle 90° (a) Velocity, (b) Temperature

Based on the simulation results as shown in Figure 14 (a) and (b), the air flow enters from the front center with varying speeds (0.25–1.5m/s), dominated by low velocity (<0.75m/s), the highest velocity (1.5m/s) is detected near the opening, while the closed area experiences flow stagnation and local eddies. The temperature distribution shows stability (27–27.25°C) in most rooms, except for the small room in the middle, which reaches 29°C. This indicates that heat transfer is even in open areas, but less than optimal in closed spaces.

Validation of Numerical and Experimental Results Values

To ensure the accuracy of the simulation results against actual data, a validation process was carried out on the temperature distribution and velocity flow values in existing building conditions. The validation results are shown in the table below, using the Root Mean Square Error method. (RMSE).

RMSE $\sqrt{\frac{\Sigma_t^n=1(A_t - F_t)^2}{n}}$

Information :

At = Actual Value (Existing Average)
Ft = Value (Simulation)
N = Amount of Data
Σ $= total\ value$

Table 3. Analysis value: Experimental and simulation temperature with RMSE

Floor	Measurement temperature (°C)	Simulation temperature (°C)	Error	Square of Error
	At	Ft	At-Ft	(At-Ft)ˆ2
1	28	28,88	-0,88	0,77
2	30	30,50	-0,50	0,25
3	32,5	31,85	0,65	0,42
			Total	0,69
			n	3
			RMSE	0,69

This means that the average error between the simulation results and the existing data is about 0.69 °C, indicating that the simulation is quite accurate compared to the actual data.

Simulation for 500 seconds shows the variation of temperature distribution and air flow in each case opening design. To assess the effectiveness of temperature reduction, an analysis was conducted on areas with a temperature below 27.15°C, then compared with the total floor area (2nd floor: 440 m², 3rd floor: 292 m²). The percentage of low-temperature areas is used as an indicator of the effectiveness of the design in improving thermal comfort, as presented in the following Figures 15, 16, and 17:

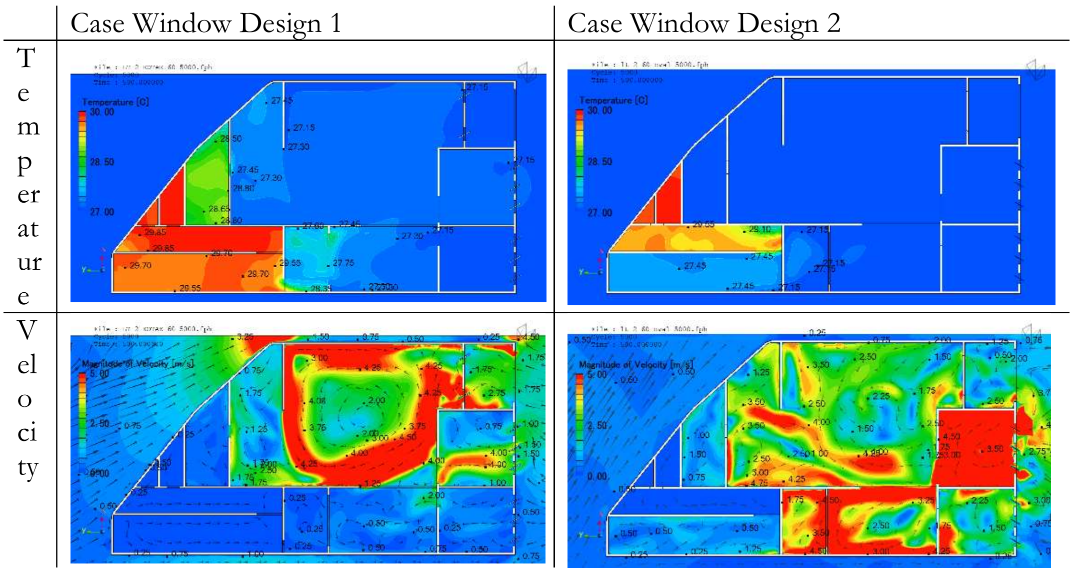

Figures 15. Comparison of Simulation Results for 2nd Floor with 60° Angle Opening

The simulation results show that the case 1 design on the 2nd floor produces a temperature area according to SNI 03-6572-2001 of 340m², while Case 2 reaches 400m². The larger area in Case 2 with a 60° opening shows more optimal thermal performance.

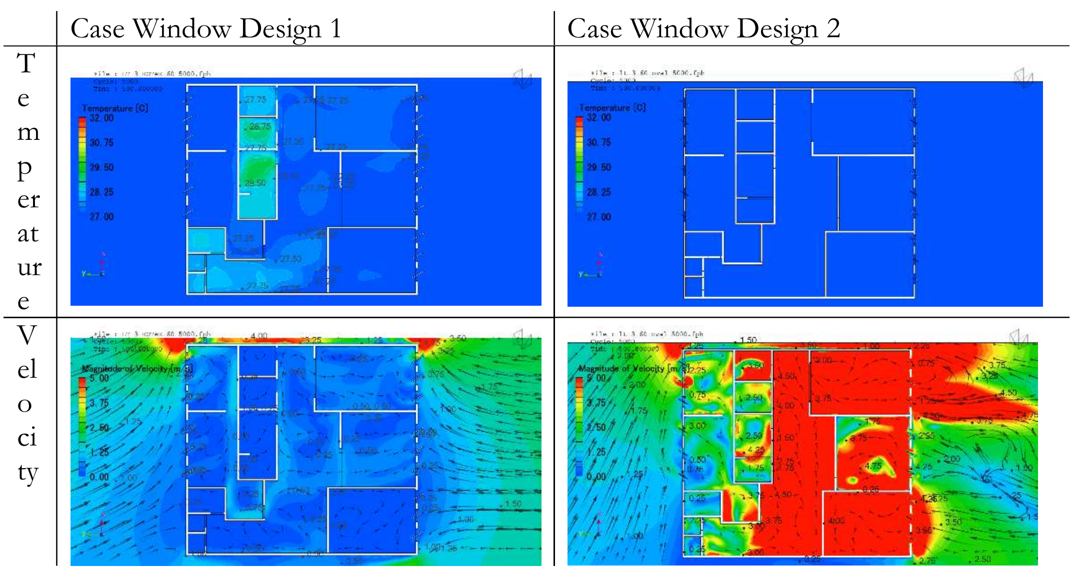

Figure 16. Comparison of Simulation Results for 3rd Floor with 60° Angle Opening

The simulation results show that the Case 1 design on the 3rd floor produces a temperature area according to SNI 03-6572-2001 of 274m², while Case 2 reaches 292m². The larger area in Case 2 with a 60° opening shows more optimal thermal performance.

	Case Window Design 1	Case Window Design 2
Temperature	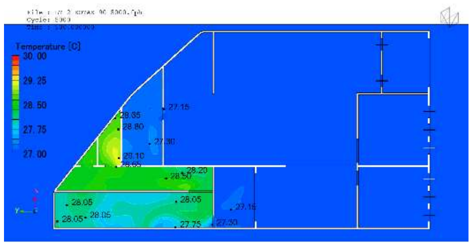	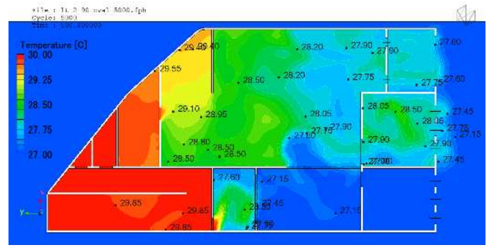
Velocity	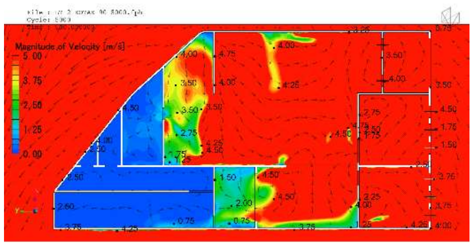	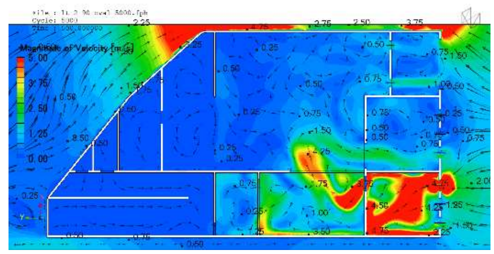

Figure 17. Comparison of Simulation Results for 2nd Floor with 90° Angle Opening

The simulation results show that the Case 1 design on the 2nd floor produces a temperature area according to SNI 03-6572-2001 of 360m², while Case 2 only reaches 60m². The larger area in Case 1 with a 90° opening shows more optimal thermal performance.

	Case Window Design 1	Case Window Design 2
Temperature	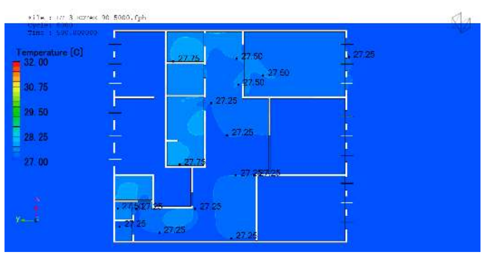	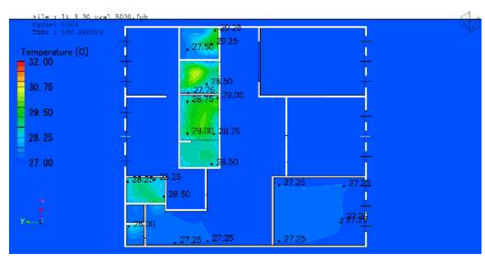
Velocity	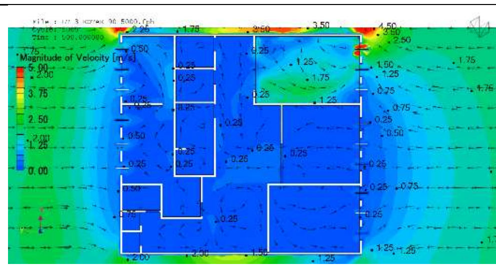	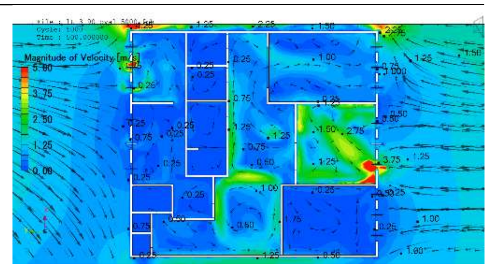

Figures 18. Comparison of Simulation Results for 3rd Floor with 90° Angle Opening

The simulation results show that the Case 1 design on the 3rd floor produces a temperature area, according to SNI 03-6572-2001, of 292m², while Case 2 has a smaller area of 256m². The larger area in Case 1 with a 90° opening shows more optimal thermal performance.

Table 4. Temperature Distribution Area

Design	Floor	Orientation Aperture	Area of temperature < 27,15°C (m²)
Case 1	2	60°	340
Case 1	3	60°	274
Case 1	2	90°	360
Case 1	3	90°	292
Case 2	2	60°	400
Case 2	3	60°	292
Case 2	2	90°	80
Case 2	3	90°	256
Total Area of Distribution of Case 1			**1.266**
Total Area of Distribution of Case 2			**1.028**

Based on Figure 18 and Table 4, Case 1 has a greater total room area with temperatures below 27.15 °C (1,266 m²), compared to Case 2, which achieves only 1,028 m². These findings indicate that Case 1 demonstrates greater effectiveness and responsiveness in generating a low temperature distribution, thereby enhancing its potential to improve thermal comfort within the room. Thus, Case 1 can be recommended as a more optimal opening design than Case 2. In addition to having better performance in low-temperature areas, the design in Case 1 is also easier to implement in terms of construction and maintenance.

Discussion

The results show that the second and third floors experienced stagnant airflow with uneven temperature distribution. Similar issues have also been noted by X. Liu et al. (2024), who reported that single-sided window ventilation often provides limited air exchange in multi-story spaces. Comparable observations were described by Cao (2019), who underlined the difficulty of relying on natural ventilation alone without carefully designed openings. The improvement observed through the use of pivot windows at 60° and 90° orientations is in line with the findings of Mora-Pérez et al. (2017), who highlighted that appropriate window configuration can enhance thermal comfort in naturally ventilated buildings. A related conclusion was presented by A. M. Rodrigues et al. (2019), who indicated that optimizing window geometry helps reduce indoor temperature variations in climates with strong solar exposure.

The finding that the square pivot window performs more effectively than the oval configuration is consistent with the observations of Sakiyama et al. (2020), who showed that geometric differences in window openings may significantly affect airflow distribution. By confirming this tendency, the present study contributes further evidence that design decisions at the level of window geometry influence ventilation performance. Finally, the validation of CFD simulation results against field measurements, with an RMSE value of 0.69, is comparable to the level of accuracy discussed by Blocken (2015), who emphasized CFD as a reliable tool for predicting ventilation when validated experimentally. Similarly, Hawendi & Gao (2017), demonstrated that CFD simulations can represent indoor airflow patterns with sufficient accuracy when supported by field validation, which strengthens the methodological basis of the present study. Overall, this study complements previous work by providing empirical evidence on the role of pivot window configurations in a tropical multi-story public building. While earlier studies such as those by X. Liu et al. (2024) and (Cao, 2019) pointed to the limitations of single-sided ventilation, the present results suggest that optimized window orientation can reduce indoor temperature and improve airflow distribution. The novelty lies in combining field measurements with CFD validation in the context of an actual library building, offering practical insights for passive design strategies in tropical regions

.

Conclusion

This study concludes that the conditions in the Pemalang Library Building on the 3rd floor indicate suboptimal air circulation and room temperature that exceed the thermal comfort threshold according to the SNI 03-6572-2001 standard. The absence of adequate ventilation results in the entrapment of hot air indoors, thereby diminishing thermal comfort for occupants. Simulation results show that the use of pivot window openings with 60° and 90° orientations, especially in square shapes, significantly increases airflow and lowers room temperature by more than 4°C compared to initial conditions. The passive ventilation design innovation was found to reduce temperatures by up to 27.1 °C in most areas of the room within a 500-second simulation, thereby confirming its effectiveness as a design solution for enhancing thermal comfort without reliance on mechanical cooling systems.

Declaration of computing interest.

The authors declare that they have no known competing financial interests or personal relationships that could have influenced the work reported in this paper.

References

Ai, Z. T., & Mak, C. M. (2016). Short-term mechanical ventilation of air-conditioned residential buildings: A general design framework and guidelines. Building and Environment, 108, 12–22. https://doi.org/10.1016/j.buildenv.2016.08.016

Albuquerque, D. P., Mateus, N., Avantaggiato, M., & Carrilho da Graça, G. (2020). Full-scale measurement and validated simulation of cooling load reduction due to nighttime natural ventilation of a large atrium. Energy and Buildings, 224, 110233. https://doi.org/10.1016/j.enbuild.2020.110233

Ali, N. M., Abd Razak, A., Mohamad, M. F., & Bahsan, R. (2017). CFD analysis on indoor temperature and velocity: Effects of incident wind angle and outlet position. Pertanika Journal of Science and Technology, 25(S7), 227–238.

Awoyera, P. O., Effiong, J., Nagaraju, V., Haque, M. A., Mydin, M. A. O., & Onyelowe, K. (2024). Alternative construction materials: a point of view on energy reduction and indoor comfort parameters. Discover Sustainability, 5(1). https://doi.org/10.1007/s43621-024-00655-y

Bachand, N., Salehipour, H., & Gorle, C. (2025). Simulating The Urban Canopy's Impact on Wind-Driven Natural Ventilation and Cooling. 2018, 1–19. http://arxiv.org/abs/2508.04091

Blocken, B. (2015). Computational Fluid Dynamics for urban physics: Importance, scales, possibilities, limitations and ten tips and tricks towards accurate and reliable simulations. Building and Environment, 91, 219–245. https://doi.org/10.1016/j.buildenv.2015.02.015

Bogdan Cfd, M., Quality, A., & Walther, E. (2017). Natural ventilation uncertainties in building energy simulations. February, 53–55. www.vaisala.com/hvac

BSN. (2001). Tata Cara Perancangan Sistem Ventilasi dan Pengkondisian Udara pada Bangunan Gedung. Sni 03-6572-2001, 1–55. https://pdfdokumen.com/download/sni-03-6572-2001-tata-cara-perencanaan-sistem-ventilasi-dan-pengkondisian-udara-pada-bangunan-gedung_5a38b43d1723dda9dc05a37e_pdf

Caciolo, M., Cui, S., Stabat, P., & Marchio, D. (2013). Development of a new correlation for single-sided natural ventilation adapted to leeward conditions. Energy and Buildings, 60, 372–382. https://doi.org/10.1016/j.enbuild.2013.01.024

Cao, S. J. (2019). Challenges of using CFD simulation for the design and online control of ventilation systems. Indoor and Built Environment, 28(1), 3–6. https://doi.org/10.1177/1420326X18810568

Chen, C., & Gorlé, C. (2022). Full-scale validation of CFD simulations of buoyancy-driven ventilation in a three-story office building. Building and Environment, 221. https://doi.org/10.1016/j.buildenv.2022.109240

Chenari, B., Dias Carrilho, J., & Gameiro Da Silva, M. (2016). Towards sustainable, energy-efficient and healthy ventilation strategies in buildings: A review. Renewable and Sustainable Energy Reviews, 59, 1426–1447. https://doi.org/10.1016/j.rser.2016.01.074

Chung-Camargo, K., González, J., Chen Austin, M., Carpino, C., Mora, D., & Arcuri, N. (2024). Advances in Retrofitting Strategies for Energy Efficiency in Tropical Climates: A Systematic Review and Analysis. Buildings, 14(6). https://doi.org/10.3390/buildings14061633

Conzatti, A., FOSAS DE PANDO, D., Chater, B., & Coley, D. (2025). Are simple models for natural ventilation suitable for shelter design? Buildings and Cities, 6(1), 158–181. https://doi.org/10.5334/bc.497

de Dear, R. J., & Brager, G. S. (2002). Thermal comfort in naturally ventilated buildings: revisions to ASHRAE Standard 55. Energy and Buildings, 34(6), 549–561. https://doi.org/https://doi.org/10.1016/S0378-7788(02)00005-1

Demir, H. (2025). Investigation on the Effect of Opening Size and Position on Wind-Driven Cross-Ventilation in an Isolated Gable Roof Building.

Elhassan, Z. A. (2023). Energy consumption performance using natural ventilation in dwelling design and CFD simulation in a hot dry climate: A case study in Sudan. Frontiers in Built Environment, 9(March), 1–14. https://doi.org/10.3389/fbuil.2023.1145747

Feeley, K. J., & Stroud, J. T. (2018). Where on Earth are the "tropics"? Frontiers of Biogeography, 10(1–2), 0–7. https://doi.org/10.21425/F5FBG38649

Ferrucci, M., & Brocato, M. (2019). Parametric analysis of the wind-driven ventilation potential of buildings with rectangular layout. Building Services Engineering Research and Technology, 40(1), 109–128. https://doi.org/10.1177/0143624418803065

Gu, Y., Cui, T., Liu, K., Yang, F., Wang, S., Song, H., Qi, Q., Meng, Q., & Li, Y. (2021). Study on influencing factors for occupant window-opening behavior: Case study of an office building in Xi'an during the transition season. Building and Environment, 200(February), 107977. https://doi.org/10.1016/j.buildenv.2021.107977

Hajdukiewicz, M., González Gallero, F. J., Mannion, P., Loomans, M. G. L. C., & Keane, M. M. (2024). A narrative review to credible computational fluid dynamics models of naturally ventilated built environments. Renewable and Sustainable Energy Reviews, 198(September 2023). https://doi.org/10.1016/j.rser.2024.114404

Haldi, F., & Robinson, D. (2008). On the behaviour and adaptation of office occupants. Building and Environment, 43(12), 2163–2177. https://doi.org/https://doi.org/10.1016/j.buildenv.2008.01.003

Hargianti, M., Nasution, N., & Hidayat, H. (2023). Infrastructure Facility Needs Analysis City Park in the New Normal Era. Jurnal PenSil, 12(3), 293–303. https://doi.org/10.21009/jpensil.v12i3.34760

Hawendi, S., & Gao, S. (2017). Impact of an external boundary wall on indoor flow field and natural cross-ventilation in an isolated family house using numerical simulations. Journal of Building Engineering, 10(March), 109–123. https://doi.org/10.1016/j.jobe.2017.03.002

Jingyuan Shi, C. Z. and Y. L. *. (2023). Angled Gable Roofs and Opening Locations.

Lee, M.-H., Kim, C.-M., Park, G.-Y., Choi, C.-H., & Park, C.-Y. (2020). [Didn't Read]Grid Independence Test of Computational Fluid Dynamics Model for Indoor Airflow Analysis. Journal of Korean Institute of Architectural Sustainable Environment and Building Systems, 14(2), 183–194.

Liu, S., Pan, W., Cao, Q., Long, Z., Jiang, Y., & Chen, Q. (2019). CFD simulations of natural cross ventilation through an apartment with modified hourly wind information from a meteorological station. Energy and Buildings, 195, 16–25. https://doi.org/10.1016/j.enbuild.2019.04.043

Liu, X., Wang, H., Li, Z., Zhao, J., Li, C., & Xie, D. (2024). Effectiveness of natural ventilation through single-sided window opening in air-conditioning rooms. Energy and Buildings, 314(November 2023), 114260. https://doi.org/10.1016/j.enbuild.2024.114260

Lü, X., Lu, T., Yang, T., Salonen, H., Dai, Z., Droege, P., & Chen, H. (2021). Improving the energy efficiency of buildings based on fluid dynamics models: A critical review. Energies, 14(17), 1–23. https://doi.org/10.3390/en14175384

M. C. Peel1, B. L. Finlayson2, and T. A. M. (2002). Updated world map of the K¨oppen-Geiger climate classification. Permafrost and Periglacial Processes, 13(3), 243–249. https://doi.org/10.1002/ppp.421

Menter, F. R. (1994). Two-equation eddy-viscosity turbulence models for engineering applications. AIAA Journal, 32(8), 1598–1605. https://doi.org/10.2514/3.12149

Mohsenzadeh, M., Marzbali, M. H., Tilaki, M. J. M., & Abdullah, A. (2021). Building form and energy efficiency in tropical climates: A case study of penang, malaysia. Urbe, 13(September). https://doi.org/10.1590/2175-3369.013.E20200280

Mora-Pérez, M., Guillen-Guillamón, I., & López-Jiménez, P. A. (2017). A CFD study for evaluating the effects of natural ventilation on indoor comfort conditions. AIMS Environmental Science, 4(2), 289–309. https://doi.org/10.3934/environsci.2017.2.289

Nisiforou, O. A., Poullis, S., & Charalambides, A. G. (2012). Behaviour, attitudes and opinion of large enterprise employees with regard to their energy usage habits and adoption of energy saving measures. Energy and Buildings, 55, 299–311. https://doi.org/10.1016/j.enbuild.2012.08.034

Palomo Amores, T., Ruda Sarria, F., Medina, D. C., Valera, T. C., Sánchez Ramos, J., & Álvarez Domínguez, S. (2025). Experimental Validation of the Potential of Cross-Ventilation Strategy as a Natural Cooling Technique Integrated in a Real Historic Building. Applied Sciences (Switzerland), 15(4). https://doi.org/10.3390/app15042174

Park, J., & Choi, C.-S. (2019). Modeling occupant behavior of the manual control of windows in residential buildings. Indoor Air, 29(2), 242–251. https://doi.org/https://doi.org/10.1111/ina.12522

Porras-Amores, C., Mazarrón, F. R., Cañas, I., & Villoría Sáez, P. (2019). Natural ventilation analysis in an underground construction: CFD simulation and experimental validation. Tunnelling and Underground Space Technology, 90(January), 162–173. https://doi.org/10.1016/j.tust.2019.04.023

Reddy, S. D. (2025). CFD Analysis on Air Conditioning Effect Using K-Omega Model.

International Journal for Research in Applied Science and Engineering Technology, 13(2), 366–378. https://doi.org/10.22214/ijraset.2025.66806

Rodrigues, A. M., Santos, M., Gomes, M. G., & Duarte, R. (2019). Impact of natural ventilation on the thermal and energy performance of buildings in a Mediterranean climate. Buildings, 9(5). https://doi.org/10.3390/buildings9050123

Rodrigues, N., Sakiyama, M., Frick, J., Bejat, T., & Garrecht, H. (2021). Parametric Modeling Approach.

Roetzel, A., Tsangrassoulis, A., Dietrich, U., & Busching, S. (2010). A review of occupant control on natural ventilation. Renewable and Sustainable Energy Reviews, 14(3), 1001–1013. https://doi.org/10.1016/j.rser.2009.11.005

Sakiyama, N. R. M., Carlo, J. C., Frick, J., & Garrecht, H. (2020). Perspectives of naturally ventilated buildings: A review. Renewable and Sustainable Energy Reviews, 130(March), 109933. https://doi.org/10.1016/j.rser.2020.109933

Sarmento, H. (2012). New paradigms in tropical limnology: The importance of the microbial food web. Hydrobiologia, 686(1), 1–14. https://doi.org/10.1007/s10750-012-1011-6

Sundell, J., Levin, H., Nazaroff, W. W., Cain, W. S., Fisk, W. J., Grimsrud, D. T., Gyntelberg, F., Li, Y., Persily, A. K., Pickering, A. C., Samet, J. M., Spengler, J. D., Taylor, S. T., & Weschler, C. J. (2011). Ventilation rates and health: Multidisciplinary review of the scientific literature. Indoor Air, 21(3), 191–204. https://doi.org/10.1111/j.1600-0668.2010.00703.x

Von Grabe, J. (2013). Flow resistance for different types of windows in the case of buoyancy ventilation. Energy and Buildings, 65, 516–522. https://doi.org/10.1016/j.enbuild.2013.06.035

Wang, H., & Chen, Q. (2012). A new empirical model for predicting single-sided, wind-driven natural ventilation in buildings. Energy and Buildings, 54, 386–394. https://doi.org/10.1016/j.enbuild.2012.07.028

Wang, L., & Greenberg, S. (2015). Window operation and impacts on building energy consumption. Energy and Buildings, 92, 313–321. https://doi.org/10.1016/j.enbuild.2015.01.060

Wen, Y., Lau, S. K., Liu, K., Xu, Z., & Leng, J. (2024). Integrating aboveground and underground environments to enhance underground natural ventilation in the tropics: Case studies in Singapore. Tunnelling and Underground Space Technology, 153(2), 106031. https://doi.org/10.1016/j.tust.2024.106031

Wen, Y., Liu, J., Dou, W., Xu, X., Cao, B., & Chen, J. (2020). Scheduling workflows with privacy protection constraints for big data applications on cloud. Future Generation Computer Systems, 108, 1084–1091. https://doi.org/10.1016/j.future.2018.03.028

Yin, X., Muhieldeen, M. W., Razman, R., Ee, J. Y. C., & Chiong, M. C. (2024). The potential effects of window configuration and interior layout on natural ventilation buildings: A comprehensive review. Cleaner Engineering and Technology, 23(October 2023), 100830. https://doi.org/10.1016/j.clet.2024.100830

Zakiah, A. (2021). Analysis of Energy-Efficient House Layout Design in Tropical Climate. DIMENSI (Journal of Architecture and Built Environment), 47(1), 11–18. https://doi.org/10.9744/dimensi.47.1.11-18

Zhu, Y., Luo, M., Ouyang, Q., Huang, L., & Cao, B. (2015). Dynamic characteristics and comfort assessment of airflows in indoor environments: A review. Building and Environment, 91, 5–14. https://doi.org/10.1016/j.buildenv.2015.03.032